

Design considerations for fiber-coupled streaked optical spectroscopy

D. S. Montgomery^{a)} and R. P. Johnson

Los Alamos National Laboratory, Los Alamos, New Mexico 87545

(Presented on 21 June 2000)

Optical fibers are used to couple light into fast time-resolved spectrometers for many applications. Here several issues arise that can seriously limit the temporal resolution, such as the wavelength dependent group delay, and intermodal dispersion. These issues are investigated in 10 m length fibers using either a 400 μm core step index or graded index fiber. A unique broadband (400–700 nm) short pulse (~ 1 ps) light source is used to measure the fiber group delay with a time-resolved spectrometer. Intermodal dispersion is also studied in these fibers using a narrow-band 1 ps pulse that is injected into the fiber with various coupling schemes, and a novel technique is employed to record the time-dependent angular mode structure. Finally, a conceptual design using ~ 100 μm core graded-index fibers is proposed for multichannel streaked optical spectroscopy on the National Ignition Facility. Designs appropriate for a low spectral resolution instrument (stimulated Raman backscattering) and a high spectral resolution instrument (stimulated Brillouin backscattering) are presented. The fiber dispersion issues are discussed in the design of these diagnostics. © 2001 American Institute of Physics. [DOI: 10.1063/1.1319603]

I. INTRODUCTION

Many applications in laser experiments require short length (several meters) optical fibers to relay optical signals to detectors with temporal resolution ≤ 50 ps, such as fast photodiodes, streak cameras, and streak camera coupled spectrometers. Although single-mode optical fibers have sufficient bandwidth to meet this requirement, the sensitivity of optical streak cameras typically requires $\sim \text{nJ}$ of energy in a time resolution element (~ 50 ps) so that power densities in excess of 100 MW/cm^2 would be needed, and nonlinear effects in the fiber become a concern. Therefore, multimode fibers are typically used for coupling to these detectors.

Several issues arise that can seriously limit the system resolution, such as the wavelength dependent group delay from broadband sources (due to refractive index), and intermodal dispersion. The group delay is often referred to as material dispersion, or group velocity dispersion (GVD) in the fiber optics literature.

For the case of streaked optical spectroscopy, the fiber dispersion characteristics can often be the limiting factor for temporal resolution. Here, the intermodal dispersion typically determines the temporal resolution, and careful choice of fiber can improve this substantially. The GVD, while large, can often be corrected with software if the spectral resolution of the system is adequate since each wavelength bin is delayed with respect to other wavelengths according to the GVD characteristics of the fiber.

Characterization of these fiber dispersion mechanisms should be considered in choosing the appropriate fiber for the design of a fiber-coupled streaked spectrometer. In this article, we report a measurement technique for determining the wavelength-dependent GVD in optical fibers. Additionally, a

novel technique is employed to measure intermodal dispersion (IMD) in fibers to determine which modes contribute most to temporal dispersion. This article is organized as follows: in Sec. II, we present measurements of the wavelength dependent GVD for 10 m lengths of both step-index and graded index optical fiber. Measurements of IMD for these fibers are presented in Sec. III for different (input) launch conditions. Conceptual designs for multiplexed fiber-coupled streaked spectrometers to measure stimulated Raman backscattering (SRS) and stimulated Brillouin backscattering (SBS) on the National Ignition Facility (NIF) are presented in Sec. IV, and the expected system performance is discussed.

II. GROUP VELOCITY DISPERSION MEASUREMENTS

Material dispersion or GVD in optical fibers arises from the wavelength dependence of the refractive index. This dispersion is important for broadband sources, and can be much larger than IMD, which depends on the core profile. However, for time-resolved spectroscopy, if the spectral resolution is sufficient then this effect can be corrected with image analysis of the time-resolved spectra. Each wavelength bin is simply delayed in time with respect to other wavelengths, and accurate characterization of the GVD and fiber length are all that is required to compensate for this effect in the measured spectra.

A broadband, short pulse (~ 1 ps) light source was produced using the $1.05 \mu\text{m}$ Ti:sapphire laser at the Los Alamos Trident laser facility.¹ The laser energy and pulse width are $\sim 500 \mu\text{J}$ and ~ 1 ps, respectively. The laser is focused with a 10 cm focal length lens into a 3 cm thick sample of SiO_2 . A slightly divergent cone of white light (~ 400 – 700 nm) is produced in the SiO_2 by self-phase modulation and forward Raman scattering.² The divergent white light is collected using a 50 mm Nikkor lens, and focused onto the optical fiber.

^{a)}Author to whom correspondence should be addressed; electronic mail: montgomery@lanl.gov

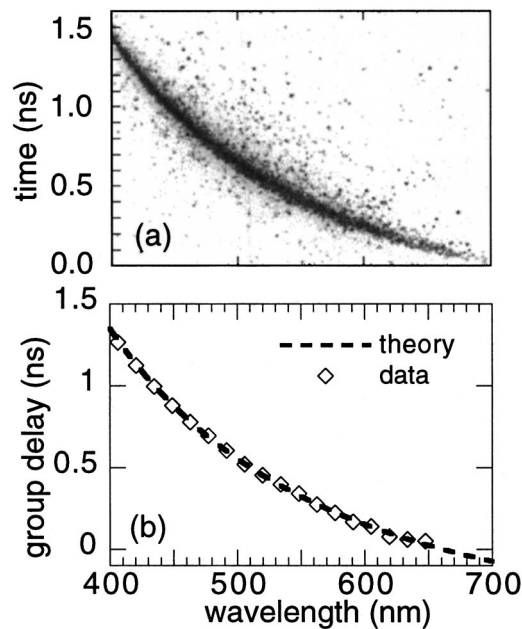


FIG. 1. (a) Step-index fiber time-resolved spectral output; (b) measured and theoretical relative group delay vs wavelength.

A Schott KG-3 filter is used to block any remaining $1.05\text{ }\mu\text{m}$ laser light, and absorbing glass filters are used to attenuate the white light. The white-light source is injected into the fiber with a $f/8$ aperture stop in the lens.

The fiber output is injected into a $f/4.5$, 0.25 m Czerny–Turner spectrometer coupled to a C4187 Hamamatsu optical streak camera. The time-resolved spectra are recorded on a Photometrics charge coupled device camera. The wavelength and time resolution of this system are $\sim 4\text{ nm}$ and 30 ps . To demonstrate that the broadband light arrived synchronously over this wavelength range, a measurement without the fiber was performed. To within the time resolution of the instrument, the broadband light is indeed synchronous.

The GVD measurements were performed separately on two commercially manufactured fibers, both $10.0 \pm 0.03\text{ m}$ in length. The first fiber is a step-index fiber with a $400\text{ }\mu\text{m}$ diam pure SiO_2 core, and a $440\text{ }\mu\text{m}$ diam cladding. The numerical aperture (NA) for the step index fiber is $\text{NA} \approx 0.22$. The second fiber is a P_2O_5 -doped SiO_2 gradient index fiber with a $435\text{ }\mu\text{m}$ diam core. The gradient profile is approximately parabolic ($\alpha \approx 2$), and the $\text{NA}^{3,4}$ is $\text{NA} \approx 0.11 \pm 0.01$. The measured attenuation for the gradient index fiber is $\approx 110\text{ dB/km}$ at 351 nm , and the transmission is expected to be greater in the visible.³ Both fibers are jacketed, and are SMA terminated and polished.

Figure 1(a) shows a streaked spectrum of the short-pulse white light source from the output of the 10 m length step-index fiber. The short wavelength portion of the spectrum arrives latest due to the higher refractive index in fused silica. The pulse width at any given wavelength is instrumentally short ($\sim 30\text{ ps}$). The time of peak emission is found for each wavelength, and the relative delay (compared to the delay at 650 nm) is measured and is plotted in Fig. 1(b).

The group delay⁵ in an optical fiber is given by $\tau_g(\lambda) = L/c[n(\lambda) - \lambda \partial n / \partial \lambda]$, where L is the fiber length (1000

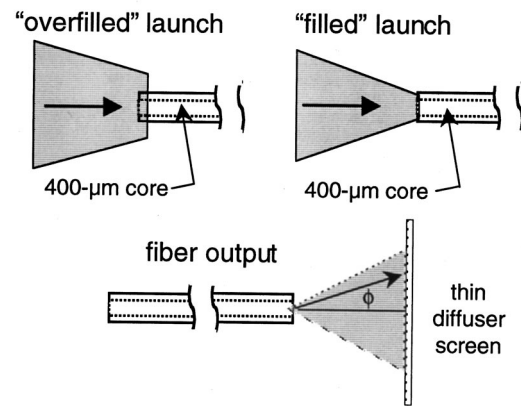


FIG. 2. Schematic of overfilled and filled fiber input launch conditions for intermodal dispersion measurements. The fiber output illuminates a thin transmissive diffuser at the streak camera slit to observe the time-dependent angular mode structure exiting the fiber.

cm), c is the vacuum speed of light, and $n(\lambda)$ is the refractive index of the fiber core material. The quantity in brackets is defined as the group index N_g . The refractive index of fused silica is determined here by the three-term Sellmeier equation.⁵ The group delay is calculated as a function of wavelength, and the delay at 650 nm is subtracted from the calculation to compare to the measurements. The theoretical group delay is overlaid in Fig. 1(b), and is in excellent agreement with the measurements. In order to obtain such good results, accurate knowledge of the refractive index of the material and the fiber length is required.

Group velocity dispersion for the $\text{P}_2\text{O}_5/\text{SiO}_2$ graded-index fiber was also measured for a 10 m length fiber. The GVD appears to be quite close but slightly greater than that measured for the SiO_2 step-index fiber, which is consistent with expected results for nominal doping levels.⁶

III. INTERMODAL DISPERSION MEASUREMENTS

A novel measurement of IMD can be performed by measuring the delay time of a narrow-band, short pulse input as a function of exit angle from the output of the fiber. Neglecting mode coupling, the lowest order modes propagate at small angles with respect to the fiber axis, and higher order modes are reflected (refracted) at larger angles. The IMD can therefore be visualized by imaging the near-field light pattern at some distance ($\sim 1\text{ cm}$) from the fiber output directly onto the slit of a streak camera so that a record of exit angle versus time can be measured. A thin, transmissive Lambertian diffuser is placed on the streak camera entrance slit so that light in high order (large angle) modes is sampled equally as low order (small angle) modes. A relatively narrow-band, short pulse light source is used to minimize effects of GVD in the measurement. A schematic of this measurement is depicted in Fig. 2. The resolution for this measurement is $\sim 30\text{ ps}$, and $\sim 0.5^\circ$ in angle.

For the $400\text{ }\mu\text{m}$ core step index fiber, the $1.05\text{ }\mu\text{m}$ Ti:sapphire laser was frequency doubled to 527 nm to produce a relatively narrow ($\sim 20\text{ }\text{\AA}$) short pulse signal to study IMD for various launching schemes in this fiber. The frequency-doubled laser illuminates a 50 mm Nikkor lens

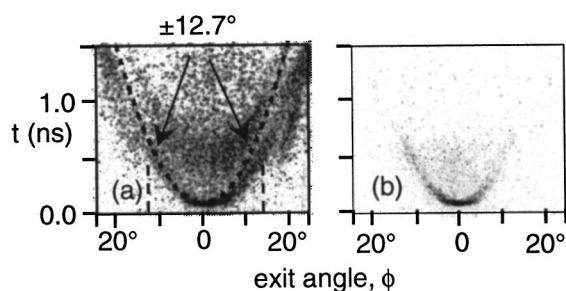


FIG. 3. Time-dependent angular measurements of IMD for an overfilled step-index fiber with: (a) $f/2$ and (b) $f/4$ input conditions. Dashed lines at $\pm 12.7^\circ$ indicate fiber NA. The dashed curve represents the theoretical IMD for this fiber.

placed sufficiently far so that its aperture is completely filled. The light is then focused onto the fiber using either an “overfilled” or a “filled” launch condition, as depicted in Fig. 2. In the overfilled launch, the laser spot size is greater than the fiber core size, and the light focuses somewhere in the fiber. This results in most of the energy in higher order modes, as determined by visually observing an annular “donut” of light on the diffuser at the fiber output. The laser spot is focused within the fiber core for the filled launch, and results in a more equal distribution of excited modes, as determined by observing a uniform “disk” of light on the diffuser. In addition, the f number of the light launched into the fiber is varied using the lens aperture stop.

Figures 3(a) and 3(b) show the angularly resolved streak of the fiber output for an overfilled launch for an input of $f/2$ and $f/4$, respectively. The measurements show that as the f number is increased, the energy output at high angle decreases, thus decreasing temporal dispersion.

The angular distribution of the fiber output was also studied for filled launch conditions. Figures 4(a) and 4(b) show the angularly resolved streak of the fiber output for filled launch conditions at $f/2$ and $f/4$. The measurements for Figs. 3 and 4 were made both with and without a diffuser placed between the Nikkor lens and the fiber input, but this did not make any significant qualitative difference.

Using a ray propagation approach, the IMD of a step-index fiber is estimated for meridional rays by $\tau_{\text{IMD}}(\phi) \approx N_g L/c[\sec(\phi/n) - 1]$, where ϕ is the exit angle, n is the refractive index, and N_g is the group index. The theoretical curve for $\tau_{\text{IMD}}(\phi)$ is overlaid in Figs. 3(a) and 4(a) for a 10 m SiO₂ step-index fiber. The signal is within $\pm 12.7^\circ$ (NA

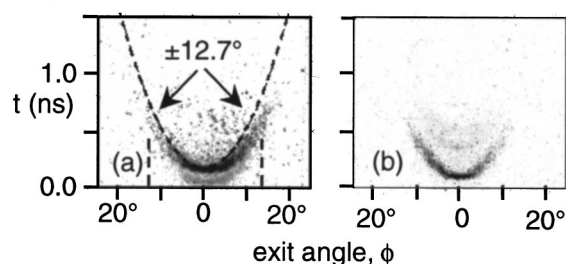


FIG. 4. Time-dependent angular measurements of IMD for a filled step-index fiber with: (a) $f/2$ and (b) $f/4$ input conditions. Dashed lines at $\pm 12.7^\circ$ indicate fiber NA. The dashed curve represents the theoretical IMD for this fiber.

$= 0.22$) for the “filled” launch, and the agreement between theory and experiment is good. The signal extends beyond the NA for the overfilled launch, which is presumably due to coupling into high-order modes in the cladding. It also appears that high-order core modes are also coupled into low order modes, as seen later in time at low exit angles. The filled launch condition at a low f number results in less mode coupling compared to the overfilled launch.

As an aside, an improvement in IMD may be realized for any detector system by coupling the fiber output to the detector using an f number that is greater than the fiber numerical aperture. This effectively rejects the higher order modes (see Figs. 3 and 4) by sampling only modes within a narrower exit cone angle, thus improving the system resolution.

IMD was also measured for a 10 m length of P₂O₅-doped graded-index fiber using the white-light source (see Sec. II) with a 90 Å wide bandpass filter centered at 551 nm. The streak data showed an angular extent of $\pm 6.1^\circ$ (NA ≈ 0.11), and the output is nearly simultaneous over this range of angles. IMD did not appear to be sensitive to different launch conditions for this fiber. The temporal width of the signal is ~ 60 ps, which is greater than the ~ 30 ps camera resolution. However, if one accounts for the GVD over the 90 Å bandwidth (~ 50 ps), then the temporal width is essentially streak camera resolution limited. The IMD at 551 nm is therefore less than 3 ps/m.

IV. CONCEPTUAL DESIGNS FOR FIBER-COUPLED STREAKED SPECTROMETERS

Both SRS and SBS are expected to occur in the backscatter direction for NIF targets. These unstable processes may significantly reduce the efficiency of energy coupled into NIF targets, and currently limit the design for ignition targets.⁷ The time-resolved spectral signatures from these processes can provide data for the local plasma conditions in which they occur, and are therefore an important measurement. Currently, up to five full-aperture backscatter stations (FABS) are planned for NIF,⁸ with each FABS measuring the backscattered energy, power, and time-resolved spectra for a four-beam quad, or up to 20 beams. Clearly, multiplexing 40 channels of time-resolved spectra (20 each for SRS and SBS) into the minimum number of detectors is advantageous due to the large expected reduction in the cost per channel.

Efficient multiplexing of several optical signals to a single streaked spectrometer can be easily achieved using optical fibers. Commercially available large-format streak cameras typically have a 25 mm long photocathode, a 40 mm diam phosphor screen, and can achieve $\sim 100 \mu\text{m}$ resolution, so that 250 spatial resolution elements and 400 temporal resolution elements can be realized. Once the spectral and temporal range and resolution for the system is specified, it is straightforward to determine the maximum number of channels that can be multiplexed into a single streaked spectrometer.

SRS is expected to occur in the wavelength range 400–700 nm for NIF plasma conditions⁷ with 351 nm laser light, and the full-scale pulse length for ignition targets is ~ 20 ns.

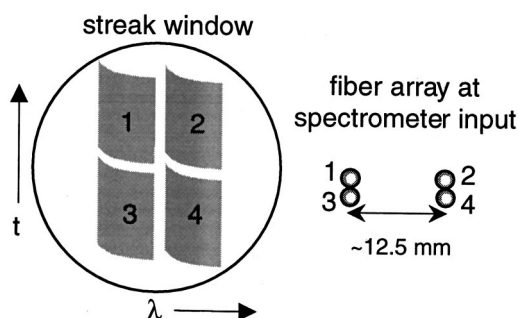


FIG. 5. Conceptual layout for fiber-multiplexed streaked spectroscopy for SRS on the NIF. The diagram on the left shows mapping of four spectral channels on streak camera output. The right diagram indicates layout of fiber array at the spectrometer input.

Using the number of resolution elements expected for commercially available streak cameras, up to four SRS spectra can easily fit within the streak camera window by offsetting the signals in space (wavelength) and time. The expected performance, based solely on the streak camera resolution, is spectral and temporal resolutions of ~ 2.5 nm and ~ 100 ps.

Figure 5 shows a conceptual layout of the spectra on the streak window. To obtain the spatial (spectral) offset, two fibers are spaced ~ 12.5 mm apart at the plane of the input slit of an imaging spectrometer. Assuming a fiber core size ≈ 50 – 100 μm , each fiber acts as its own virtual slit which is offset spatially with respect to the other fiber, and produces two side-by-side spectra for a broadband source, as depicted in Fig. 5. Two additional spectra are recorded using fibers located vertically adjacent to the other two fibers, and a time delay of ~ 20 ns can be introduced to temporally offset these spectra by using longer fibers. The schematic also depicts the wavelength varying delay in each spectrum due to GVD in the fiber. Overlap of the spectra in the time direction due to GVD can be avoided by using shorter length fibers, otherwise the number of temporally multiplexed signals or the time resolution must be reduced if longer fibers are necessary.

An example system that could meet the specifications for SRS is a 250 mm focal length Czerny–Turner spectrometer with a 120 groove/mm grating, which produces a linear spectral dispersion of ≈ 25 nm/mm. For fiber core sizes ≤ 100 μm , the spectral resolution would be streak camera limited at ~ 2.5 nm for 100 μm spatial resolution. A nominal streak camera sweep speed of 1 ns/mm would allow two sets of spectra to be temporally multiplexed with ~ 100 ps resolution over 20 ns full scale for each spectrum. Phosphosilicate graded-index fibers, such as discussed in Sec. III, are commercially available with $\text{NA} \approx 0.12$ for 50–100 μm core sizes, and should have ~ 1 ps/m IMD,³ and ≈ 150 ps/m GVD over the wavelength range 400–700 nm. Therefore, up to 50 m of fiber can be used for each spectral channel before the temporal resolution is substantially degraded.

The expected wavelength range for SBS occurs over 3480–3540 Å for NIF plasma conditions.⁷ Since the SBS spectra are slightly shifted from the laser wavelength, high

spectral resolution is required. Following the example given for SRS, it is possible to multiplex up to eight spectral channels per streaked spectrometer (four in spectrum, two in time) with a spectral and temporal resolution of 1 Å and 100 ps for each channel. Fibers for each spectral channel would be separated by ~ 6 mm, assuming a linear spectral dispersion of 10 Å/mm. An example of a system that could meet the specifications for SRS is a 750 mm focal length Czerny–Turner spectrometer with a 1000 groove/mm grating. The fiber lengths will be limited to ≈ 50 – 100 m before IMD³ (0.5–1.0 ps/m) degrades the temporal resolution. GVD is not as severe for this relatively narrow-band wavelength range.

One additional consideration in the system performance for this high-resolution spectrometer is the time shear due to diffraction,⁹ which is given by $\Delta t = GSm \cdot \lambda / c$, where G is the grating groove density (grooves/mm), S is the grating size (mm), m is the spectral order, λ is the average wavelength (μm), and c is the speed of light (≈ 300 $\mu\text{m}/\text{ps}$). If the spectrometer acceptance is $f/8$ (~ 100 mm grating size), then the time shear is substantial, ~ 120 ps. By simply increasing the spectrometer f number ($f/15$, 50 mm grating) the time shear can be reduced to ~ 60 ps. Higher spectral resolution can be achieved using a higher dispersion grating, but careful consideration of the grating size must be taken into account so that temporal resolution is not degraded. At some point, the spectral resolution will be degraded beyond the streak camera spatial resolution limit with increasing f number, and a trade-off between spectral and temporal resolution must be considered. Increasing the spectrometer f number to decrease the time shear will also decrease the spectrometer throughput, and can potentially increase stochastic noise in the measurement, and must also be considered.¹⁰

ACKNOWLEDGMENTS

The authors acknowledge useful discussions with G. Kyrala at LANL, C.E. Thompson at LLNL, and W. Seka and A.V. Okishev at the University of Rochester. This work was performed under the auspices of the U.S. Department of Energy by LANL under Contract No. W-7405-ENG-36.

¹N. K. Moncur, R. P. Johnson, R. G. Watt, and R. B. Gibson, *Appl. Opt.* **34**, 4274 (1995).

²M. Wittmann and A. Penzkofer, *Opt. Commun.* **126**, 308 (1996).

³C. E. Thompson (private communication).

⁴A. V. Okishev (private communication).

⁵J. A. Buck, *Fundamentals of Optical Fibers* (Wiley, New York, 1995).

⁶Donald B. Keck, in *Fundamentals of Optical Fiber Communications*, edited by Michael K. Barnoski (Academic, New York, 1981).

⁷J. D. Lindl, *Phys. Plasmas* **2**, 3933 (1995).

⁸R. J. Leeper *et al.*, *Rev. Sci. Instrum.* **68**, 868 (1997).

⁹N. H. Schiller and R. R. Alfano, *Opt. Commun.* **35**, 451 (1980).

¹⁰For an incoherent source, as the effective f number of the spectrometer is increased, the time resolution increases linearly with f (number of coherence times $\sim 1/f$), and the effective number of coherence regions sampled by the detector decreases as $\sim 1/f^2$. The stochastic variance goes as the product of the number of independent spatial and temporal coherence samples, so the stochastic signal-to-noise decreases as $1/f^{3/2}$. For a more complete description, see J. W. Goodman, *Statistical Optics* (Wiley, New York, 1985).